Noble metal nanodisks epitaxially formed on ZnO nanorods and their effect on photoluminescence

Sheng Chu,[1] Jingjian Ren,[1] Dong Yan,[2] Jian Huang,[1] and Jianlin Liu[1,a)]
[1]*Quantum Structures Laboratory, Department of Electrical Engineering, University of California, Riverside, California 92521, USA*
[2]*Center for Nanoscale Science and Engineering, University of California, Riverside, California 92521, USA*

(Received 8 April 2012; accepted 13 July 2012; published online 27 July 2012)

Triangular and hexagonal shaped noble metal (Au, Ag, Pt, Pd) nanodisks were synthesized on the top facets of ZnO nanorods via simple deposition-annealing method. Other metals (Ni, Cu, Cr, Pb, Al) only formed irregular shaped nanostructures on ZnO nanorods. The morphology, elemental composition, as well as growth mechanism of the metal nanodisks/ZnO nanorod composite materials were studied. The localized surface plasmon resonant effects from different metal nanodisks on the photoluminescence of ZnO nanorods were investigated. It was demonstrated that the carriers transfer between the metal nanodisks and ZnO can efficiently manipulate the photoluminescence intensities from the nanorods. © *2012 American Institute of Physics*. [http://dx.doi.org/10.1063/1.4739516]

Noble metal nanostructures, such as Au and Ag, exhibit prominent response to electromagnetic fields because of their strong surface plasmon resonance (SPR), which is induced by the resonant oscillation of surface electrons when illuminated with light of appropriate wavelength.[1–4] On the other hand, being promising for compact light sources and energy efficient devices, semiconducting nanowires/nanorods have been extensively studied and much insight has been achieved on tuning their electrical and optical properties by controlling their sizes and dimensions.[5,6] For example, quasi 1D nanowires/nanorods are found to be important optical gain media and low-cost resonant cavity, which have enabled laser emissions.[7–12] Recently, progress on electrically pumped waveguide lasing in ZnO nanowires has been made via Fabry-Perot[8] and whispering gallery modes.[9]

Hybrid composite materials generated through integrating metal nanoparticles directly on semiconductor nanowires/nanorods may represent a promising class of functional materials, since the coupling between the metal nanoparticles and semiconductors will induce novel optical, electronic, and magnetic properties. For instance, metal nanoparticle decorations can boost nanowire solar cells' efficiencies because noble metal nanoparticles with suitable sizes can be strongly excited by solar irradiation and the excited electrons can be injected into the conduction band of semiconductors;[13] on ZnO thin films, various metal nanoparticles have been used to effectively adjust the near band edge (NBE) emission by coupling the SPR states to excitons in ZnO.[14–16] In principle, properties of metal/semiconductor hybrid materials are strongly dependent on the properties of the metal nanoparticles, such as their shapes.[17] Morphology controlled metal nanoparticles are often synthesized through solution based chemistry methods,[18,19] e-beam lithography,[20] as well as nanosphere lithography.[21] Although the shape control and production rate are to certain level satisfactory, they could not offer the placement of those nanoparticles on desired semiconductor nanostructures with high-quality interface, which is critical to electronic charge transfer, minimization of non-radiative recombination, as well as the reliability of the composite materials. Although the growth of metal nanodisks with anisotropic morphologies on semiconductor wafers was studied by a few researchers,[22,23] limited progress has been made to realize such nanostructures on semiconductor nanorods.

In this paper, we report a simple approach for the self-epitaxy of triangular/hexagonal metal (Au, Ag, Pt, Pd) nanodisks on the top end facets of c-oriented ZnO nanorods. The nanodisks' composition and structure and epitaxial relationship between the metal nanocrystals and ZnO were thoroughly investigated and determined. The SPR effects from metal nanodisks were utilized to manipulate the light emission in the hybrid system. Among various metals, Ag nanodisks decoration on ZnO nanorods exhibited strongest photoluminescence (PL) under the excitation by 325 nm laser.

High-quality ZnO nanorods were synthesized in a tube furnace, the detailed growth procedure can be found elsewhere.[8] The as-grown nanorods are single crystal, having smooth surfaces at the top end facets. Metals (Au, Ag, Pt, Pd, Al, Ni, Pb, Cu, Cr) with nominal thickness of 1 nm were deposited in a common e-beam evaporator at room temperature under a vacuum pressure of $\sim 10^{-7}$ Torr. After taken out from the deposition chamber, all samples were immediately subjected to rapid thermal annealing at 700 °C for 60 seconds (s) in N_2 environment in order to enable the formation of nanodisks. Figures 1(a) and 1(b) show the morphology of Au on ZnO before and after annealing, respectively. As seen from Fig. 1(a), random shaped nano-islands instead of continuous film formed on the as-deposited sample, due to the metal's high surface tension.[24] Gaining enough energy under annealing, the Au nano-islands changed their morphology drastically afterwards: neatly oriented hexagonal thin nanodisks with dimensions 20–50 nm formed on top of the nanowire's end surface. In the mean time, smaller random shaped nano-dots were found on the side facets of ZnO nanorods. The growth of hexagonal shaped nanodisks suggests that Au atoms become mobile by annealing, and the self-organized epitaxy of Au on certain ZnO facet should be responsible for the closely parallel hexagonal sidewall facets of these two materials. X-ray energy dispersive spectroscopy (EDS) with

a)jianlin@ee.ucr.edu.

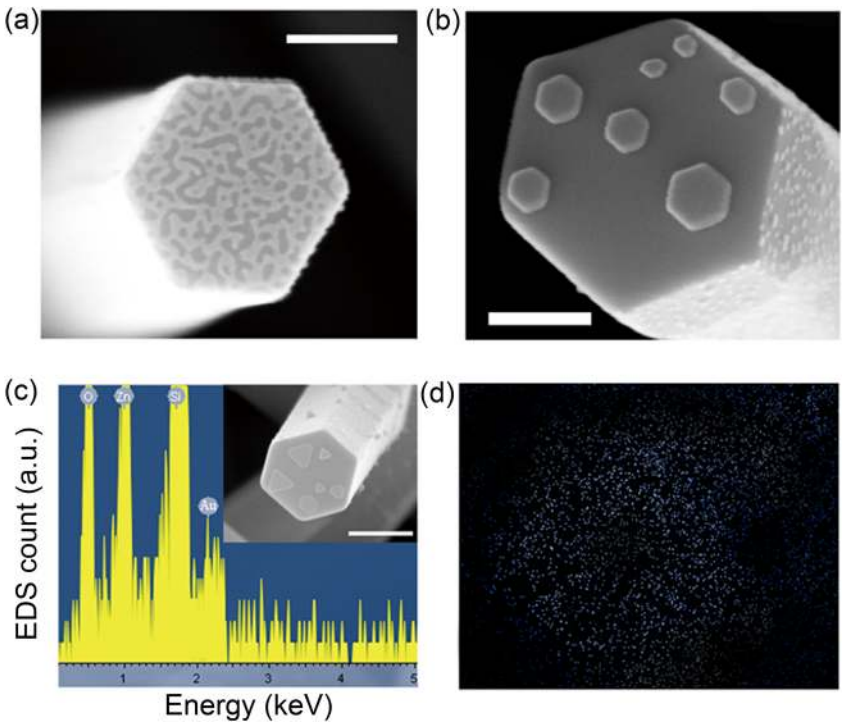

FIG. 1. (a) SEM image of as-deposited Au on ZnO nanorods. (b) SEM image of annealed Au nanodisks. Scale bars: 100 nm. (c) EDS spectrum of the Au nanodisk-coated ZnO nanorod shown in the inset. (d) EDS mapping signal of the sample.

mapping capability from a Carl Zeiss Leo SUPRA 55 system was employed to confirm the elemental composition in the metal nanodisks. Figures 1(c) and 1(d) show the EDS spectrum and the mappings of Au signal, respectively, for the sample shown in the inset of Fig. 1(c). As seen from Fig. 1(c), Au_M signal is found around 2.15 keV. Meanwhile, despite the relatively weak Au signal due to large penetration depth of the electron beam (1.5 μm under 20 kV acceleration), it is confirmed that the location of majority Au can be reasonably linked to the nanodisks areas on the corresponding nanowire' top facet.

The nanodisk's atomic structure and interface crystallinity were investigated by a Philips Tecnai 12 transmission electron microscope (TEM). Figure 2 shows a TEM image of multiple nanodisks (darker contrast) on the top facet of a ZnO nanorod. It is noted that smaller and irregular shaped nano-dots are also seen on the sidewall of the nanorod, which suggests that in these areas, the matched epitaxial growth (between Au and ZnO) tendency is much weaker. The left inset shows the fast Fourier transform (FFT) analysis of the periodicity of the crystal planes, which indicates that two sets of lattices were recorded. The 2.55 Å lattice spacing comes from typical ZnO (0002) planes and the 2.35 Å one is assigned to Au (111) (inter-plane distance 2.36 Å). Selected area electron diffraction (SAED) pattern in the right inset provides additional crystallography information. Indexes of lattice diffractions that associate with Au and ZnO are marked. From the configuration of ZnO's patterns, it can be interpreted that the electron beam incidence direction is along ZnO [0100] direction, while the Au related pattern is a typical result of electron diffraction from $[11\bar{2}]$ direction.[25] Based on these observations, the lattice relationship image of Au nanodisks on ZnO can be constructed as follows: Au [111] || ZnO [0002] and Au $[11\bar{2}]$ || ZnO [0100].

Several other noble metals (Ag, Pt, Pd) can also form similar shaped nanodisks from the same method, as shown in Figures 3(a)–3(c), respectively. The growth of these regular metal nanodisks apparently undergoes Volmer-Weber (VW) mode. The formation process is therefore dominated by minimizing the total energy, in which the interface energy induced by strain plays a very important role. For example, in the case of three fold symmetric Au (111) plane matching on six fold ZnO (0001) plane (shown in Fig. 3(h)), the lattice constant a of the Au (111) plane is 2.88 Å, while the a for ZnO (0001) plane is 3.25 Å, so 12.8% mismatch is calculated. Similarly, the in-plane lattice constants for face centered cubic (FCC) metals Ag, Pt, Pd on the (111) plane are 2.89, 2.77, and 2.75 Å, respectively. As a result, the strains

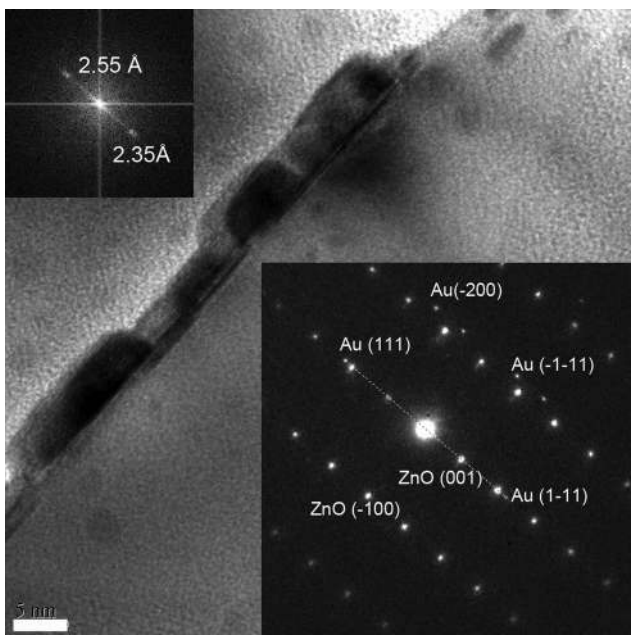

FIG. 2. TEM image of the Au nanodisks on ZnO nanorod. Scale bar: 5 nm. Left inset: FFT analysis of the structure, showing two lattice parameters. Right inset: SAED pattern of the Au/ZnO structure.

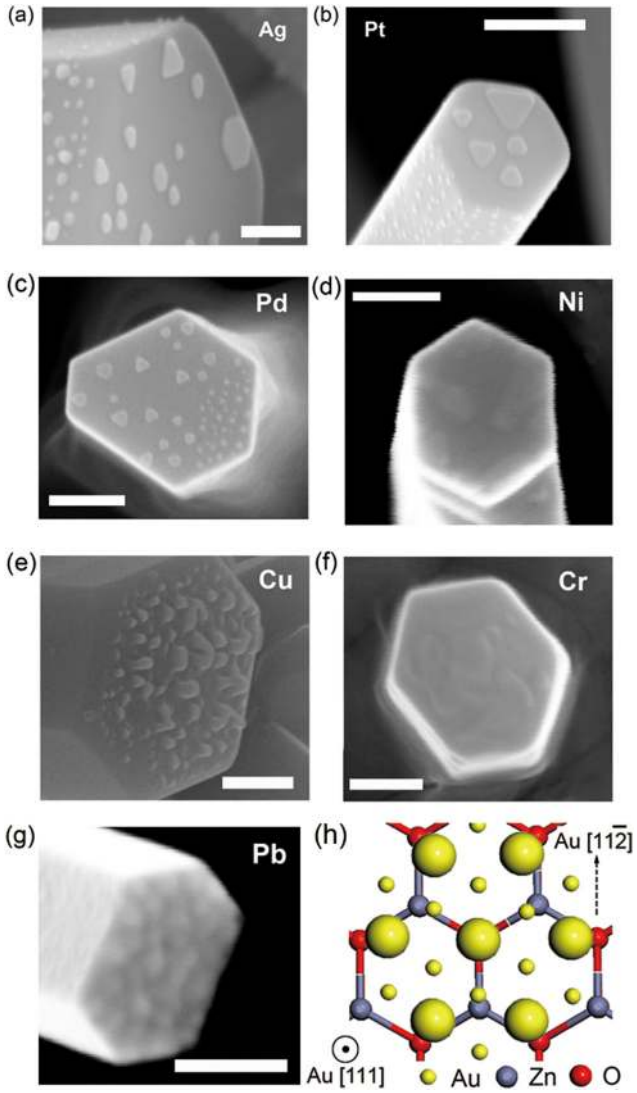

FIG. 3. SEM image of (a) Ag, (b) Pt, (c) Pd, (d) Ni, (e) Cu, (f) Cr, (g) Pb coated ZnO nanorods after annealing. Scale bars: 100 nm. (h) Schematic of the Au atoms on ZnO (0001) surface. Large green balls represent Au atoms on the interface plane.

for these corresponding metals on ZnO (0001) are 12.4%, 17.1%, and 18.1%. Obviously, all the mismatches are very large, which cannot be sustained in mesoscopic cases, but they could be tolerable for nanostructures. Other metals (Ni, Cu, Cr, Pb) were also used in our experiment (Figures 3(d)–3(g)). These elements either have too large strain (Ni-30.4%, Cu-27.3%) or have compressive strain (Cr-18%, Pb-7.1%), resulting in unfavorable and isotropic shaped nano-islands growth. The summary of various metal elements with corresponding lattice constant is shown in Figure 4. The elements that have the tendency to form regular nanodisks are marked as green balls. Generally, green balls fall into the center area in white color (with approximate 20% mismatch as the limit). Nevertheless, one exception was found in the metal Al. Although Al (FCC structure) has a relatively small lattice mismatch of 13.5% with ZnO (0001) plane, it does not form regular shaped nanodisks (blue cross in Figure 4), which might be due to the rapid reaction and oxidation of Al nanostructures with ZnO.[26]

A number of reports have demonstrated the possibility of using noble metal nanoparticles to enhance NBE emission

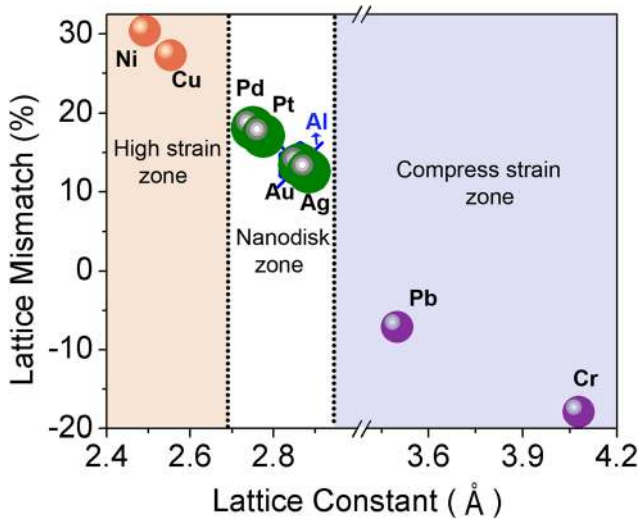

FIG. 4. Plot of lattice mismatch between metal and ZnO (0001) as a function of metal elements' lattice constant. Green balls indicate the metals that can form well-defined shapes.

in ZnO.[14–16] Under the irradiation with light having a wavelength larger than the particle size, the high-density electrons on the noble metal nanoparticles form an electron cloud and oscillate. If the noble metal nanoparticles are connected with ZnO, the electrons accumulate at the interface between the metal and ZnO may have a chance to transfer to ZnO side, whose rate is determined by interface band bending as well as the coupling between surface plasmons and exciton states in ZnO. Here, similar energy transfer mechanism is utilized to manipulate the luminescence properties of ZnO excited by He-Cd laser with 325 nm line, while the effects from different noble metal nanodisks are examined.

To gain more insight into the optical enhancement by the metal nanodisks, three dimensional finite difference time domain (FDTD) method was first used to simulate the absorption characteristics of different nanodisks. To simplify the simulation, five nanodisks with uniform thickness of 8 nm, but with different diameters and shapes were employed, in order to represent the distribution of nanodisks' dimensions (inset of Figure 4). The simulated absorption spectra for selected metals Au, Ag, Pd, Pt are shown in Figure 5(a). Other metals are not included in this plot due to their inability of formation of triangular and hexagonal shaped nanodisks. It is inferred that the response for different elements varies drastically due to their unique SPR effects. At the target wavelength of 325 nm, Au and Ag have significantly higher absorption cross section than the others. Hence, the electrons in the SPR states may absorb greater amount of photons, which can resonate with exciton's energy and transfer to ZnO to form NBE emissions. To experimentally demonstrate optical emission enhancement of ZnO nanorods by metal nanodisks coating, the vertically aligned ZnO nanorods were grown, followed by polymethyl methacrylate (PMMA) covering the sides of nanorods before metal deposition. The sample was cut into pieces and e-beam evaporation was used to cover each piece with different metals (Au, Ag, Pt, Pd). The samples were annealed after the PMMA removal and subjected to laser excitation. The PMMA process used here allows us to prevent the metal deposition on the

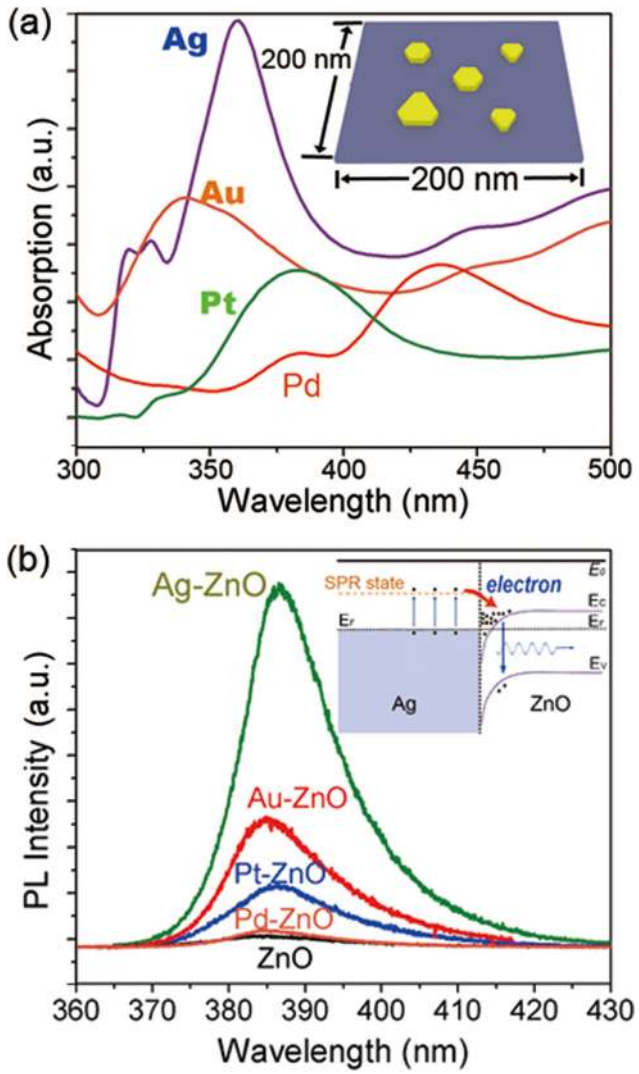

FIG. 5. (a) FDTD simulation results of absorption spectra of Au, Ag, Pt, Pd nanodisks. Inset is the schematic of the FDTD simulation environment. (b) PL spectra of Ag, Au, Pt, Pd metal nanodisks decorated ZnO nanorods and a sample without metal nanodisk coating. Inset: schematic band diagram of the metal/ZnO interface.

sidewalls of the nanorods and to only focus on the effect of metal nanodisks at the top facets of the nanorods on their optical properties. Figure 5(b) shows PL spectra of the samples. All metal nanodisk-coated samples exhibit higher emission intensity than the reference ZnO nanorod without any coating. The emission intensities increase over one magnitude due to the incorporation of Au and Ag nanodisks, which is consistent with the FDTD simulation result. In addition, the PL intensity of Ag nanodisk decorated sample is much greater than that of Au nanodisk coated sample because the band bending and contact behaviors may have additional effects on electron transfer ability.[27] Since the electron affinity of ZnO (4.35 eV) is larger than the work function of Ag (4.26 eV), an electron well is formed in the Ag/ZnO interface due to band bending of ZnO and it will be easy for the electrons to transfer from Ag to ZnO, as illustrated in the inset of Figure 5. On the other hand, even if Au absorbs more light at 325 nm than Ag does, due to its large work function of 5.1 eV, the electrons will have to overcome a barrier before entering ZnO, leading to downgraded transfer rate and slightly weaker emission.

In summary, Au, Ag, Pt, Pd metal nanodisks with well-defined shapes have been synthesized on top of ZnO nanorods surface through simple deposition-annealing methods. Other metals such as Ni, Cu, Cr, Pb, Al only formed random-shaped structures on ZnO nanorods. The formation mechanism of these nanostructures has been characterized. The application of nanodisks on the enhancement of NBE emissions in ZnO nanorods was investigated and large tunability of emission intensities was achieved. This research provides a method of creating multi-elemental plasmonic nanostructures on semiconductor nanorod surfaces, which may pave the way for many applications.

This work was supported by NSF (EECS-0900978). The authors appreciate valuable discussion on self-assembled quantum dot growth mechanism with Dr. Hao Hu from Material Science and Engineering in University of Utah. The authors thank Dr. Krassimir Bozhilov in UCR CFAMM for TEM assistance.

[1]J. N. Anker, W. P. Hall, O. Lyandres, N. C. Shah, J. Zhao, and R. Van Duyne, Nature Mater. **7**, 442 (2008).
[2]L. M. Liz-Marzan, Mater. Today **7**, 26 (2004).
[3]S. A. Maier and H. A. Atwater, J. Appl. Phys. **98**, 011101 (2005).
[4]M. I. Stockman, Phys. Today **64**(2), 39 (2011).
[5]R. Yan, D. Gargas, and P. Yang, Nature Photon. **3**, 569 (2009).
[6]Y. Li, F. Qian, J. Xiang, and C. M. Lieber, Mater. Today **9**, 18 (2006).
[7]M. H. Huang, S. Mao, H. Feick, H. Yan, Y. Wu, H. Kind, E. Weber, R. Russo, and P. Yang, Science **292**, 1897 (2001).
[8]S. Chu, G. Wang, W. Zhou, Y. Lin, L. Chernyak, J. Zhao, J. Kong, L. Li, J. Ren, and J. Liu, Nat. Nanotechnol. **6**, 506 (2011).
[9]J. Dai, C. X. Xu, and X. W. Sun, Adv. Mater. **23**, 4115 (2011).
[10]S. Gradecak, F. Qian, and C. M. Lieber, Appl. Phys. Lett. **87**, 173111 (2005).
[11]B. L. Cao, Y. Jiang, and C. Wang, Adv. Funct. Mater. **17**, 1501 (2006).
[12]T. Wang, F. Ranalli, and P. J. Parbrook, Appl. Phys. Lett. **86**, 103103 (2005).
[13]Y. Tian and T. Tatsuma, J. Am. Chem. Soc. **127**, 7632 (2005).
[14]M. Lee, T. Kim, W. Kim, and Y. Sung, J. Phys. Chem. C **112**, 10079 (2008).
[15]S. G. Zhang, X. W. Zhang, Z. G. Yin, J. X. Wang, J. J. Dong, H. L. Gao, F. T. Si, S. S. Sun, and Y. Tao, Appl. Phys. Lett. **99**, 181116 (2011).
[16]X. H. Xiao, F. Ren, X. D. Zhou, T. C. Peng, W. Wu, X. N. Peng, X.F. Yu, and C. Z. Jiang, Appl. Phys. Lett. **97**, 071909 (2010).
[17]C. J. Murphy, T. K. Sau, A. M. Gole, C. J. Orendorff, J. Gao, L. Gou, S. E. Hunyadi, and T. Li, J. Phys. Chem. B **109**, 13857 (2005).
[18]Y. Sun, B. Mayers, and Y. Xia, Adv. Mater. **15**, 641 (2003).
[19]T. Herricks, J. Chen, and Y. Xia, Nano. Lett. **4**, 2367 (2004).
[20]G. J. Leggett, ACS Nano **5**, 1575 (2011).
[21]J. C. Hulteen and R. P. Van Duyne, J. Vac. Sci. Technol. A **13**, 1553 (1995).
[22]Y. Sun, Adv. Funct. Mater. **20**, 3646 (2010).
[23]M. Aizawa, A. M. Cooper, M. Malac, and J. M. Buriak, Nano. Lett. **5**, 815 (2005).
[24]M. Jose-Yacaman, C. Gutierrez-Wing, M. Miki, D. Q. Yang, K. N. Piyakis, and E. Sacher, J. Phys. Chem. B **109**, 9703 (2005).
[25]J. Wang, M. Tian, T. E. Mallouk, and M. H. W. Chan, J. Phys. Chem. B **108**, 841 (2004).
[26]M. J. Meziani, C. E. Bunker, F. Lu, H. Li, W. Wang, E. A. Guliants, R. A. Quinn, and Y. P. Sun, ACS Appl. Mater. Int. **1**, 703 (2009).
[27]Y. J. Fang, J. Sha, Z. L. Wang, Y. T. Wan, W. W. Xia, and Y. W. Wang, Appl. Phys. Lett. **98**, 033103 (2011).